International Journal of Energy Research

INTERNATIONAL JOURNAL OF ENERGY RESEARCH
Int. J. Energy Res. 2014; **38**:714–727
Published online 23 July 2013 in Wiley Online Library (wileyonlinelibrary.com). DOI: 10.1002/er.3076

Exergetic analysis of a desiccant cooling system: searching for performance improvement opportunities

Pedro Gonçalves[1,*,†], Giovanni Angrisani[2], Maurizio Sasso[2], Adélio Rodrigues Gaspar[1] and Manuel Gameiro da Silva[1]

[1]ADAI-LAETA, Department of Mechanical Engineering, University of Coimbra, Rua Luís Reis Santos, Pólo II, 3030-788 Coimbra, Portugal
[2]DING, Università degli Studi del Sannio, Piazza Roma 21, 82100 Benevento, Italy

SUMMARY

The current increase of the energy consumption of buildings requires new approaches to solve economic, environmental and regulatory issues. Exergy methods are thermodynamic tools searching for sources of inefficiencies in energy conversion systems that the current energy techniques may not identify. Desiccant cooling systems (DCS) are equipments applied to dehumidifying and cooling air streams, which may provide reductions of primary energy demand relatively to conventional air-conditioning units. In this study, a detailed thermodynamic analysis of open-cycle DCS is presented. It aims to assess the overall energy and exergy performance of the plant and identify its most inefficient sub-components, associated to higher sources of irreversibilities. The main limitations of the energy methods are highlighted, and the opportunities given by exergy approach for improving the system performance are properly identified. As case study, using a pre-calibrated TRNSYS model, the overall energy and exergy efficiency of the plant were found as 32.2% and 11.8%, respectively, for a summer week in Mediterranean climate. The exergy efficiency defect identified the boiler (69.0%) and the chiller (12.3%) as the most inefficient components of the plant, so their replacement by high efficient systems is the most rational approach for improving its performance. As alternative heating system to the boiler, a set of different technologies and integration of renewables were proposed and evaluated applying the indicators: primary energy ratio (PER) and exergy efficiency. The heating system fuelled by wood was found as having the best primary energy performance (PER = 109.6%), although the related exergy efficiency is only 11.4%. The highest exergy performance option corresponds to heat pump technology with coefficient of performance (COP) = 4, having a PER of 50.6% and exergy efficiency of 28.2%. Additionally, the parametric analyses conducted for different operating conditions indicate that the overall irreversibility rate increases moderately for larger cooling effects and more significant for higher dehumidification rates. Copyright © 2013 John Wiley & Sons, Ltd.

KEY WORDS

desiccant cooling systems; exergy efficiency; exergy efficiency defect; renewable energy sources

Correspondence

*Pedro Gonçalves, ADAI-LAETA, Department of Mechanical Engineering, University of Coimbra, Rua Luís Reis Santos, Pólo II, 3030-788 Coimbra, Portugal.
†E-mail: pedro.goncalves@dem.uc.pt

Received 23 September 2012; Revised 21 May 2013; Accepted 3 June 2013

1. INTRODUCTION

The exergy analysis is a thermodynamic analysis technique based on second law of thermodynamic that provides an alternative way for assessing and comparing processes and systems more rationally and meaningfully. This well-known technique is defined as a measure of the potential work of different energy forms or states evaluated in a given reference environment [1–3]. The method may be applied to any thermodynamic system, and in particular for multi-component systems, it is able to identify and locate irreversibility sources, allowing to evaluate the contribution of each subsystem for the overall inefficiency of the plant [4].

Regarding to achieve comfort indoor environmental conditions, active energy systems are usually installed in buildings. Nevertheless, due to their high energy consumption, operating costs and/or some harmful effects on environment, these systems have been replaced by alternative ones, including hybrid systems that make use of renewable energy resources. Despite most of conventional systems are strongly implemented, most of their alternatives are still under research or development stages. The desiccant cooling systems (DCS) are heat-driven systems, designed to provide cooled and dehumidified air to indoor environments, and have been moderately applied as alternative or complement to conventional compression/absorption

cooling systems. These systems could have potentially economic, energy and environmental advantages with respect to traditional cooling devices, although the complexity of such systems may reduce their acceptance, especially in situations where there aren't on-site qualified operating professionals. Its operation is based on a rotary dehumidifier (the desiccant wheel, DW), where the air is dehumidified. It is made by a desiccant material, such as silica gel, activated alumina or lithium chloride salt, which is able to hold the moisture of the air. Although, it has to be regenerated through a warm air stream, usually heated by a gas fired boiler. Low-grade thermal energy (60–95 °C) is sufficient for the regeneration, meaning that solar, geothermal or waste heat may be used. Previously dehumidified and after passing through an air-to-air heat exchanger, the air stream can be cooled to the desired temperature, forcing it to cross a cooling coil (connected to a conventional chiller, for example). A DCS may avoid the air stream of overcooling and re-heating, as occurs in the conventional systems providing cooled and dehumidified air.

Several research works involving DCS have been conducted in the last years. Angrisani *et al*. [5–8] conducted a set of experimental-based studies on a small-scale poly-generation system, constituted by a natural gas microcogenerator connected to a DCS. The authors assessed all technical features of all the sub-components of a DCS system and successfully implemented and calibrated it into a model, developed in TRNSYS [9]. Parmar *et al*. [10] developed an artificial neural network model for predicting the dry bulb temperature and specific air humidity at the outlet of a DW. La *et al*. [11] studied a modified regenerative evaporative cooling system coupled to a rotary desiccant cooling process, which can produce both dry air and chilled water simultaneously. The authors aimed to evaluate the feasibility and energy-saving potential of this novel system. Combining chilled ceiling, displacement ventilation and desiccant dehumidification, Hao *et al*. [12] investigated the feasibility of this integrated system for finding the configuration that can realize desirable levels of indoor air quality, thermal comfort and energy savings in hot and humid climates.

From all the studies reviewed [5–12], they are based on an entirely energy conventional (or first law of thermodynamic) approach, not revealing the actual thermodynamic performance of the systems under analysis and not answering to questions, such as: 'How far each system is from ideal system?'; or 'What is the most inefficient component of the plant?'; or even 'How much each system contributes for the plant inefficiency?'. These and other questions, may be answered using exergy methods that have been applied as valuable tools for design, analysis or performance assessments of different type of systems: solar thermal systems [13,14], cogeneration systems [15,16], buildings and HVAC systems [17,18], power and refrigeration cycles [19,20]; or even in large scale, such as societies or countries [21].

Using the second law analysis, Darwish *et al*. [20] investigated a liquid-phase separation novel refrigeration cycle, concluding that the highest inefficient component is the heating generator, contributing to the total exergy destruction of the plant in 42%. Roux *et al*. [14] conducted a thermodynamic optimization of a small-scale solar thermal Brayton cycle, dividing inefficiency sources into two types of irreversibilities (internal and external), finding that the internal irreversibility rate is almost three times the external irreversibility rate. Wei *et al*. [22] presented an exergy analysis study of variable air volume system for office buildings air-conditioning, and concluded that the largest improvement on exergy efficiency is obtained by changing the heating source from electricity to renewable energy sources (such as solar or geothermal), closing that the use of mechanical cooling in cold climate should be more questioned. The benefits of exergy analysis combined with dynamic energy simulation tools were also claimed by Wei *et al*. [22], which suggested the integration of the exergy methods into building energy codes (such as EnergyPlus [23] or TRNSYS [9]).

Specifically, in the field of DCS, few studies on exergy analysis have been found in literature: Lavan *et al*. [24] assessed the overall second law performance for a desiccant air-conditioning system, applying the concept of 'feasible performance'. Additionally, Kanoglu *et al*. [25] developed a procedure for energy and exergy analysis of DCS. The authors found that DW has the greatest percentage of exergy destruction followed by the heating system. These analyses allowed to quantify and identify the sites with the losses of exergy and therefore showing the direction to approach the ideal coefficient of performance (COP). And Hurdogan *et al*. [26] evaluated the energy–exergy performance of a novel DCS, using average measured parameters obtained from experimental results. The exergy efficiencies of all the systems components were determined in an attempt to assess their individual performances and found the improvement potential. In the field of liquid desiccant dehumidification systems, the studies [27–29] were also performed.

From the reviewed studies about DCS [24–26], the authors have applied exergy analysis to assess in detail the exergy performance or locate irreversibility sources, although without considering other technologies or sources for the heating system (e.g. solar thermal, heat pump, wood-based systems, etc). Also the evaluation of the impact of replacing one of components on the exergy performance of other components or plant as a whole was not discussed.

In this study, the exergy method was implemented into a pre-calibrated DCS model, previously implemented in TRNSYS by Angrisani *et al*. [7,30]. The objective is to assess the overall energy and exergy performance of all components and DCS plant as a whole and locate the most inefficient components, associated to higher sources of irreversibilities. As case study, using weather data corresponding to the city of Naples (Italy), for the period from 1st to 7th August (9 h00–18 h00), the indicators primary energy ratio (PER), exergy efficiency, irreversibilities rate, exergy efficiency defect and relative irreversibility were assessed and discussed. Additionally, PER and exergy efficiency were assessed and compared for a set of renewable energy scenarios and different heating technologies (e.g. solar thermal, wood-fuelled heating systems and

heat pumps). The main irreversibilities present in the DCS were evaluated as function of the operating conditions during the period. At the end, an iso-line diagram was proposed for evaluating irreversibilities savings due to improvements on boiler efficiency or integration of renewables from solar thermal.

2. THE EXERGY METHOD APPLIED TO DCS

In DCS, moist air is exposed to several changes of temperature and humidity ratio, so special attention should be given to the exergy variations of moist air in each system component. The definition of the reference dead state is also a very sensitive parameter in exergy analysis and should be carefully treated. According to Ref. [1], the specific exergy of a mixture air flow is constituted by a thermo-mechanical and chemical exergy component, generically described by Eq. (1).

$$ex = ex_{tm} + ex_{ch} \tag{1}$$

where ex_{tm} is the thermo-mechanical exergy, and ex_{ch} is related to the chemical exergy term, which are related to the change from the actual state to a restricted or dead state. Neglecting kinetic and potential effects, the thermo-mechanical exergy and chemical exergy are given by Eqs. (2) and (3), respectively [1],

$$ex_{tm} = (h - h_0) - T_0(s - s_0) \tag{2}$$

$$ex_{ch} = \sum_{i=1}^{n} y_i(\mu_i - \mu_{i,0}) \tag{3}$$

where, in Eq. (2), h is the specific enthalpy, s the specific entropy and T_0 is the dead-state temperature. In Eq. (3), y_i and μ_i are the molar fraction of substance in the mixture and the chemical potential of the substance i, respectively, and the sub-script '0' represents the restricted dead-state point.

2.1. Specific exergy of moist air and water

Assuming the outdoor air as an ideal gas mixture, constituted by dry air and water vapour, the exergy of moist air at a given point j, neglecting kinetic and potential effects, is given by Eq. (4) [1].

$$ex_j = \underbrace{(c_{p,a} + \omega c_{p,v})\left[T_j - T_0 - T_0 \ln\left(\frac{T_j}{T_0}\right)\right]}_{thermal} + \underbrace{(1 + 1.608\omega_j) R_a T_0 \ln\left(\frac{p_j}{p_0}\right)}_{mechanical} + \underbrace{R_a T_0\left[(1 + 1.608\omega_j)\ln\left(\frac{1 + 1.608\omega_0}{1 + 1.608\omega_j}\right) + 1.608\omega \ln\left(\frac{\omega_j}{\omega_0}\right)\right]}_{chemical} \tag{4}$$

where $c_{p,a}$ and $c_{p,v}$ are the specific heat of dry air and water vapour at constant pressure, ω_j and ω_0 are the humidity ratio of moist air at point j and dead-state point, respectively; T_j and T_0 are the temperature at point j and dead state, respectively. R_a is the ideal gas constant of dry air and p_j and p_0 are the pressure at point j and dead state, respectively. The specific exergy of water at point j is described by Eq. (5) [1].

$$ex_{w,j} = \underbrace{(h_{f,j} - h_{f,0}) - T_0(s_{f,j} - s_{f,0})}_{thermal} + \underbrace{v_f(p_j - p_{sat})}_{mechanical} - \underbrace{R_v T_0 \ln\varphi_0}_{chemical} \tag{5}$$

where, the symbols $h_{f,j}$ and $h_{f,0}$ are the specific enthalpy of saturated liquid at a generic point j and at dead state, respectively; $s_{f,j}$ and $s_{f,0}$ are the specific entropy of saturated liquid at a generic point j and at dead state, respectively. T_0 is the dead-state temperature, v_f is the specific volume of liquid water, p_j and p_{sat} are the pressure at a generic point j and saturated pressure, respectively. R_v is the universal constant for the water vapour (ideal gas), and φ_0 is the relative humidity at dead state. For water flows in closed-cycle circuits, without any contact with air, the chemical term $R_v T_0 \ln\varphi_0$ becomes zero, since it is assumed $\varphi_0 = 1$ (saturated state). For applications with steam injector, where pure water enters or leaves the control volume (e.g. evaporative coolers), φ_0 is calculated for the air properties at dead-state point.

2.2. Exergy-based indicators

In engineering systems, non-dimensional energy ratios are usually applied to evaluate energy systems efficiencies (e.g. the thermal efficiency or coefficient of performance, COP). It gives information about 'the ability to produce a desired effect with minimum use of energy or resource' [2]. However, the efficiency based on a purely a energy approach is ambiguous and cannot accurately measure 'the distance' to ideal (reversible) system. Therefore, the performance of a given energy system should be evaluated by means of exergy or second law efficiency. A general definition of exergy efficiency for a given k component is given by Eq. (6).

$$\psi_k = \frac{\dot{E}x_{out,k}}{\dot{E}x_{in,k}} = 1 - \frac{\dot{I}_k}{\dot{E}x_{in,k}} \tag{6}$$

where $\dot{E}x_{out,k}$ and $\dot{E}x_{in,k}$ are the exergy output and input rate to the component k, respectively, and $\dot{I}_k$ is the irreversibility rate generated at component k. The symbols $\dot{E}x_{out,k}$ and $\dot{E}x_{in,k}$ could not represent physical input/outputs rates, but desired or required effects. The ratio of exergy output to exergy input is always less than unit and its value depends on the degree of irreversibility of the process, which is a particular suitable

Int. J. Energy Res. 2014; **38**:714–727 © 2013 John Wiley & Sons, Ltd.
DOI: 10.1002/er

criterion for the degree of thermodynamic perfection of a process [3].

In a multi-component system like a DCS, where the control volume can be divided into a finite number of sub-systems, there are advantages to introduce the concepts of 'exergy efficiency defect' (δ) and relative irreversibility (I_R). Exergy efficiency defect is given by the ratio between exergy destruction rate at the k-th component to the total exergy input rate to the overall system, as given by Eq. (7) [3].

$$\delta_k = \frac{\dot{I}_k}{\sum \dot{E}x_{in,k}} \tag{7}$$

The relative irreversibility, $I_{R,k}$ is defined by the ratio of exergy destruction of the k-th component to the total irreversibility rate occurring in the system, as shown by Eq. (8).

$$I_{R,k} = \frac{\dot{I}_k}{\sum_k \dot{I}_k} \tag{8}$$

The sum of the exergy efficiency defect of the k components is expressed by Eq. (9), where ψ_{ove} is the overall efficiency of the system, showing the direct causal relationship between component's irreversibility rate and their effect on overall efficiency of the system.

$$\sum_k \delta_k = 1 - \psi_{ove} \tag{9}$$

Finally, the comparison of irreversibilities levels between systems may be done through the indicator relative irreversibilities savings (RIS) [31], expressed by

$$RIS_k = 1 - \frac{\dot{I}_k}{\dot{I}_{k,ref}} \tag{10}$$

where $\dot{I}_k$ are the irreversibility rate for a given heating system, and $\dot{I}_{ref}$ is the irreversibility rate for the reference scenario.

3. METHODOLOGY

3.1. System description

The DCS system under study is an air handling unit located at the Università degli Studi del Sannio in Benevento (Italy), constituted by a DW, an air-to-air heat exchanger, an evaporative cooler and heating and cooling coils. A natural gas boiler is used as heating system for the DW regeneration and the (additional) sensible cooling of the process air exiting the cross flow heat exchanger is performed by a conventional chiller. The schematic of the system is shown in Figure 1, where three air flows (R, C and P) are represented:

- 'Stream R' is used for the regeneration of the DW (5–6) after its passage in the heating coil interacting with the boiler (1–5);
- 'Stream C' is the auxiliary air flow used for the pre-cooling of the processed air (7–8) after its passage in the evaporative cooler (1–7);
- 'Stream P' is the process air, dehumidified by the DW (1–2), pre-cooled at the cross flow heat exchanger (2–3) and cooled at the cooling coil (3–4), which interacts with the chiller.

The assessment points (1–13) are presented in Figure 1, where point no. 1 represents the outdoors conditions. In Refs [5–8], more detailed information about the

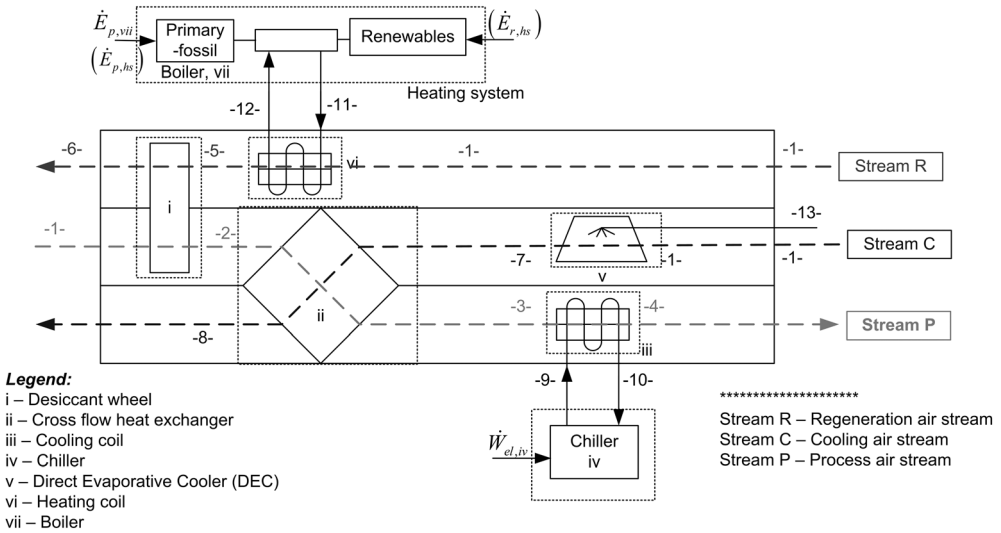

Figure 1. Schematic of the desiccant cooling system.

experimental plant lay-out is available. The TRNSYS model of the DCS was calibrated and validated using experimental data by Angrisani *et al.* [7] and implemented in [30]. The main parameters used for each DCS component (Type in TRNSYS) are presented in Table I.

3.2. Energy and exergy methods applied to DCS

In this study, for the energy and exergy analysis of the DCS system described in Figure 1, the following assumptions were taken into account:

a) Steady-state and one-dimensional condition;
b) Negligible potential and kinetic energy effects;
c) No pressure losses across the components;
d) The auxiliaries loads for the fans and pumps were neglected.

According to Figure 1, the system was divided in seven components (i–vii), and 13 assessed points (1–13), where the specific energy and exergy were evaluated. In Eqs. (11–17) [26], a set of equations describing mathematical formulations for energy and exergy-based performances of the components *i–vii* are shown [25,26]:

DW, *i*:

$$\begin{cases} \epsilon_i = \dfrac{\dot{m}_{a,P}(\omega_1 - \omega_2)h_{fg}}{\dot{m}_{a,R}(h_5 - h_1)} \\ \psi_i = \dfrac{\dot{m}_{a,P}(ex_2 - ex_1)}{\dot{m}_{a,R}(ex_5 - ex_6)} \end{cases} \tag{11}$$

Heat exchanger, *ii*:

$$\begin{cases} \epsilon_{ii} = \dfrac{\dot{m}_{a,P}c_{p,a}(T_2 - T_3)}{\dot{C}_{\min}(T_2 - T_7)} \\ \psi_{ii} = \dfrac{\dot{m}_{a,C}(ex_8 - ex_7)}{\dot{m}_{a,P}(ex_2 - ex_3)} \end{cases} \tag{12}$$

Cooling coil, *iii*:

$$\begin{cases} \epsilon_{iii} = \dfrac{\dot{m}_{a,P}c_{p,a}(T_3 - T_4)}{\dot{C}_{\min}(T_3 - T_9)} \\ \psi_{iii} = \dfrac{\dot{m}_{a,P}(ex_3 - ex_4)}{\dot{m}_{cw}(ex_9 - ex_{10})} \end{cases} \tag{13}$$

Chiller, *iv*:

$$\begin{cases} COP_{iv} = \dfrac{\dot{m}_{cw}(h_9 - h_{10})}{\dot{W}_{el,iv}} \\ \psi_{iv} = \dfrac{\dot{m}_{cw}(ex_9 - ex_{10})}{\dot{W}_{el,iv}} \end{cases} \tag{14}$$

Evaporative cooler, *v*:

$$\begin{cases} \epsilon_v = \dfrac{(T_1 - T_7)}{T_1 - T_{w,1}} \\ \psi_v = \dfrac{\dot{m}_{a,C}ex_7}{\dot{m}_{a,C}ex_1 + \dot{m}_{w,13}ex_{w,13}} \end{cases} \tag{15}$$

Heating coil, *vi*:

$$\begin{cases} \epsilon_{vi} = \dfrac{\dot{m}_{a,P}c_{p,a}(T_5 - T_1)}{\dot{C}_{\min}(T_{11} - T_1)} \\ \psi_{vi} = \dfrac{\dot{m}_{a,R}(ex_5 - ex_1)}{\dot{m}_{hw}(ex_{11} - ex_{12})} \end{cases} \tag{16}$$

Natural gas boiler, *vii*:

$$\begin{cases} \eta_{vii} = \dfrac{\dot{m}_{hw}(h_{11} - h_{12})}{\dot{E}_{p,vii}} \\ \psi_{vii} = \dfrac{\dot{m}_{hw}(ex_{11} - ex_{12})}{F^{ex}_{f,vii}\dot{E}_{p,vii}} \end{cases} \tag{17}$$

The symbol h_{fg} is the enthalpy of vaporization for water, ω is the humidity ratio, h is the specific enthalpy

Table I. The main parameters of the TRNSYS types used for the components models under investigation.

Component	Type no.	Parameter	Value
i	1716	Dehumidifier F1 effectiveness [-]	0.207
		Dehumidifier F2 effectiveness [-]	0.717
		Set-point outlet air humidity ratio [kg/kg]	0.008
ii	91	Heat exchanger effectiveness [-]	0.446
iii	508	Coil bypass fraction [-]	0.177
		Set-point outlet air temperature [°C]	18.0
iv	655	Rated capacity [kW]	8.45
		Rated COP [-]	2.93
v	506	Saturation efficiency [-]	0.551
vi	670	Effectiveness of heat exchanger [-]	0.842
vii	6	Maximum heating rate [kW]	26.7
		Efficiency of auxiliary heater [-]	0.902

and *ex* is the specify exergy. $\dot{m}_{a,P}$, $\dot{m}_{a,R}$ and $\dot{m}_{a,C}$ are the air mass flow rate for stream P, R and C, respectively. $\dot{m}_{hw}$ $\dot{m}_{cw}$ are the hot and cold water mass flow rate, respectively. $F^{ex}_{f,vii}$ is the chemical exergy to Lower Heating Value (LHV) (quality factor) of the fuel (natural gas), which in this study was assumed equal to 1.04, according to Ref. [3]. $\dot{E}_{p,vii}$ is the primary-fossil energy input (natural gas) and $\dot{W}_{el,iv}$ is the electric power input to the chiller (equivalent to exergy). In Eq. (11), the effectiveness related to the DW is defined as the ratio between the dehumidification performance of the wheel with respect to the regeneration heat input. In Eqs. (12), (13) and (16), the effectiveness related to components *ii*, *iii* and *vi*, respectively, is given as the ratio of the amount of heat transfer to the maximum possible heat transfer, where $\dot{C}_{\min}$ is the minimum of the capacitance rate of cold and hot streams, given by the product of mass flow rate and specific heat related to each stream. COP is the coefficient of performance of the chiller, and η_{hs} is the thermal efficiency of the boiler.

The overall energy performance of the DCS is defined by PER, which is defined by the ratio of cooling capacity to the total primary-fossil energy inputs, as expressed in Eq. (18).

$$PER_{ove} = \frac{\dot{m}_{a,P}(h_1 - h_4)}{\underbrace{\dot{E}_{p,vii}}_{boiler} + \underbrace{F^{p}_{el}\dot{W}_{el,iv}}_{chiller}} \tag{18}$$

where, $\dot{E}_{p,vii}$ is the primary energy input to the boiler, given by the product of fuel mass flow rate to the LHV of fuel. In this study, natural gas is assumed as primary energy source. For electricity, the conversion factor for primary-fossil energy F^{p}_{el} is calculated based on the average electric grid efficiency. In this paper, $F^{p}_{el} = 2.17$, calculated for the efficiency of Italian electric grid, η_{eg} = 46.1% [32]. Concerning the overall exergy efficiency of the system, ψ_{ove}, it is calculated through Eq. (9).

3.3. Energy–exergy performances and integration of renewables

The heat required for DW regeneration could be provided from both renewable and fossil energy sources. Depending on required temperature levels, only some type of renewable sources could be used for the regeneration process of DW, so renewables combined with fossil powered systems are commonly used. As an example, solar thermal systems are usually combined with boilers or heat pump systems. On the other side, combustion-based renewable systems, fuelled by wood, pellets or others biofuels, may be used as stand-alone (single) heating system, once they could provide enough air temperature for DW regeneration.

When renewables are included, the demand for primary-fossil energy is reduced, leading to an increase of the energy performance of the system (PER). Thus, for a given fraction of heat delivered from renewables, (ϕ_r), the corresponding primary energy demand of a fuel-based heating system $\dot{E}_{p,hs}$ is generically obtained by

$$\dot{E}_{p,hs} = \frac{\dot{Q}_{reg}}{\eta_{hs}}(1 - \phi_r) \tag{19}$$

where $\dot{Q}_{reg}$ is the heat required for the regeneration, and η_{hs} is the overall thermal efficiency of heating system. For electric-based heating systems, the value given by Eq. (19) should be multiplied by F^{p}_{el}, which is the primary conversion factor related to electricity.

Concerning the assessment of total exergy input when renewables are included into the heating system, the exergy input rate is formulated by

$$\dot{E}x_{hs} = F^{ex}_{f,hs}\dot{E}_{p,hs} + F^{ex}_{r,hs}\dot{E}_{r,hs} \tag{20}$$

where, $\dot{E}_{p,hs}$ and $\dot{E}_{r,hs}$ are fossil and renewable source energy inputs, respectively, and $F^{ex}_{f,hs}$ and $F^{ex}_{r,hs}$ are the exergy to LHV ratio of the fossil and renewable fuels, respectively. Concerning renewable sources, if direct thermal sources are used (e.g. hot water from solar thermal), $F^{ex}_{r,hs}$ is commonly calculated by Eq. (21) [33].

$$F^{ex}_{r,hs} = 1 - \frac{T_0}{(T_s - T_r)}\ln\left(\frac{T_s}{T_r}\right) \tag{21}$$

where T_s and T_r are the supply and return temperature, respectively, and T_0 is the dead-state temperature.

4. RESULTS AND DISCUSSION

In this section, the energy and exergy results derived from the simulations of the DCS model [30] are presented. Averaged values for temperature, humidity ratio, dry air/water mass flow rate and power inputs, calculated for the period from 1st to 7th August, from 9 h00 to 18 h00 and using

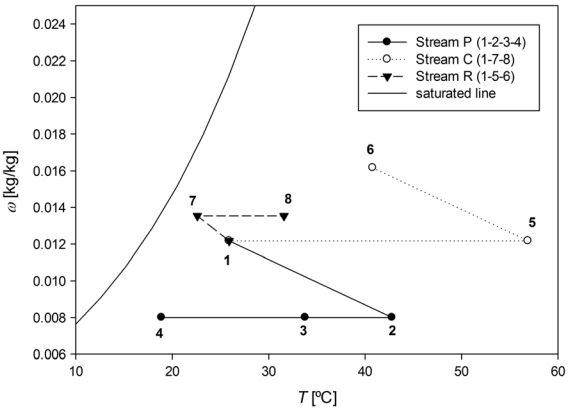

Figure 2. Evolution of the temperature and humidity ratio for the points of the stream P, C and R.

climate data corresponding to the city of Naples (Italy), were used to perform the analyses. In this period, the outdoor temperature varies from 21 to 29 °C and the humidity ratio from 0.008 to 0.017 kg of water/kg dry air.

The evolution of humidity ratio and dry bulb temperature for the air points (1–8) of the DCS is shown in Figure 2. where the saturated line corresponding to the moist air with 100 % humidity ratio is also represented. In air stream P (air points 1–2–3–4), water vapour is removed from the air by means of the DW (1–2); two constant humidity ratio cooling processes then follows: one at cross flow heat exchanger (2–3), and the other at cooling coil (3–4). In air stream C, water vapour is added by means of the evaporative cooler (1–7); a heating process (7–8) at heat exchanger then follows. Finally, as regards the regeneration air stream R, the air flow is heated in the heating coil (1–5), before passing through the DW (5–6).

4.1. Dead-state point

An important issue in exergy analysis is the definition of the dead-state point, which describes conditions where the specific exergy is zero. In the literature on exergy analysis of DCS, there is no recommended value for the definition of the dead-state condition, although this is a very important issue and should be carefully chosen. For this study, the median of outdoor temperature and humidity ratio that occurs in the period from 1st to 7th August (9 h00 to 18 h00) was chosen as dead state, regarding to be the nearest point to the environmental conditions during the operation of the plant. Using the climate file corresponding to the city of Naples (Italy), the dead state was found as: $T_0 = 26.1$ °C, $\omega_0 = 0.0114$ kg water/kg dry air, ($\varphi_0 = 53.5\%$). The pressure (dead state) was assumed constant for all points assessed, $p_0 = 101.325$ kPa, so the mechanical part of exergy in Eq. (4) is neglected by this study.

4.2. Energy and exergy properties

The evolution of the specific exergy of moist air at each point of streams P, C and R is shown in Figure 3.

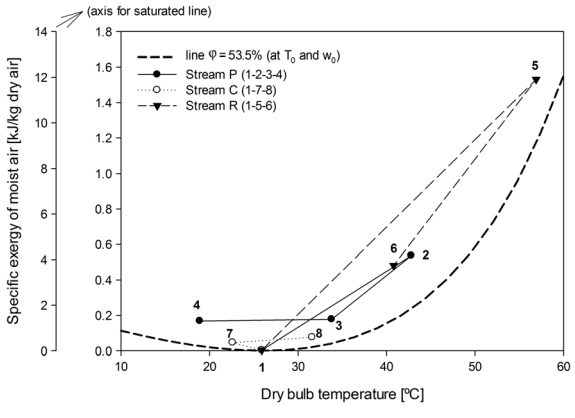

Figure 3. Evolution of the specific exergy with dry bulb temperature at each point of the stream P, C and R.

Comparing the exergy variation of the three main air streams, stream R has the highest point's exergy variation, followed by stream P and C. Points in stream C are near environmental conditions or dead-state point, therefore their specific exergy are near zero. Furthermore, the isoline at $\varphi_0 = 53.5\%$ is represented, having the lowest value (zero) at dead-state conditions.

The numeric values of temperature, humidity ratio, enthalpy and specific exergy of the points (1–13) in DCS are presented in Table II. The specific enthalpy of moist air and specific enthalpy/entropy of water, required by Eq. (5), were calculated by means of Engineering Equation Solver software package [34]. Additionally, thermal and chemical exergy components (Eq. (4)) of moist air points are also presented in Table II, as well as the fraction related to thermal exergy (ratio of specific thermal exergy to total specific exergy). As expected, higher fractions of thermal exergy occur for high deviations of air temperatures relatively to dead-state temperature (Points 2 and 5). For points particularly near to the dead-state temperature (Points 1, 3, 4 and 7), the specific exergy of moist air is mostly equally divided in thermal and chemical exergy. As stated, since the pressure differences related to dead state were neglected, the mechanical component of exergy was ignored.

Some special attention is given for specific exergy of the water points (9–12) and (13), which differs in one magnitude order. Thus, in the points (9–12), only thermomechanical aspects were assumed, because as points in a closed circuit, without air contact, a saturated atmosphere is assumed ($\varphi_0 = 1$), and $R_v T_0 \ln \varphi_{0s} = 0$. Nevertheless, the water spray used for air humidification (13), both thermomechanical and chemical exergy of water should be taken into account, since $\varphi_0 \neq 1$.

4.3. Energy and exergy performances

The individual operation of each component allows to identify and quantify the sites where the exergy destruction (irreversibilities) occurs showing the direction to approach the best plant performance (or reversible COP). In this section, the energy- and exergy-based results for each individual component and plant as a whole are presented.

The parameter commonly applied to assess the energy-based performance of heat exchangers, DW or evaporative cooler is the effectiveness. On the other hand, for the boiler and chiller, parameters such as thermal efficiency and COP are currently applied. Furthermore, these energy-based performances influence the exergy performances and the related irreversibilities rates. The differences between energy-based and exergy efficiencies of each DCS component are shown in Figure 4. The effectiveness of DW presents the lowest energy-based performance, while chiller and boiler have higher energy efficiencies, followed by the heating and cooling coils, with values of 75% and 84%, respectively. The chiller has a COP estimated in the period of 2.37, while the boiler has a constant thermal efficiency of 90.2%. The overall PER of the DCS has a value of 32.2%, showing that there are potential for improving

Int. J. Energy Res. 2014; **38**:714–727 © 2013 John Wiley & Sons, Ltd.
DOI: 10.1002/er

Table II. Air and water properties used for exergy analysis.

Fluid [point]	Temperature [°C]	Humidity ratio [kg/kg dry air]	Specific enthalpy [kJ/kg]	Mass flow rate (kg/s)	Specific exergy [kJ/kg]	Specific thermal exergy [kJ/kg]	Specific exergy (chemical) [kJ/kg]	Ratio of thermal exergy to total exergy
Air [0]	26.1	0.0114	55.4	-	0.000	0.000	0.000	0.000
Air [1]	25.9	0.0122	57.2	0.225	0.004	0.000	0.004	2%
Air [2]	42.8	0.0080	63.5	0.225	0.536	0.459	0.077	85%
Air [3]	33.8	0.0080	54.5	0.225	0.176	0.099	0.077	56%
Air [4]	18.9	0.0080	39.3	0.225	0.167	0.090	0.077	53%
Air [5]	56.9	0.0122	89.1	0.225	1.531	1.527	0.004	100%
Air [6]	40.8	0.0162	82.8	0.225	0.483	0.362	0.121	75%
Air [7]	22.6	0.0135	57.1	0.225	0.046	0.021	0.025	47%
Air [8]	31.6	0.0135	66.4	0.225	0.076	0.051	0.025	68%
Water [0]	26.1	-	109.4	-	0.000	n.a.	n.a.	n.a.
Water [9]	13.9	-	58.4	0.404	1.070	n.a.	n.a.	n.a.
Water [10]	16.0	-	67.2	0.404	0.729	n.a.	n.a.	n.a.
Water [11]	62.7	-	262.5	0.165	8.661	n.a.	n.a.	n.a.
Water [12]	52.3	-	219.0	0.165	4.534	n.a.	n.a.	n.a.
Water [13] (spray)	22.6	-	94.8	0.001	82.630	n.a.	n.a.	n.a.

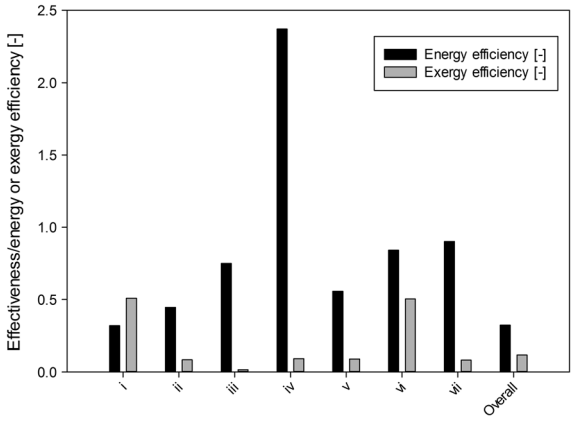

Figure 4. Energy and exergy-based efficiencies of sub-components of DCS and overall system.

PER. Questions such as: 'where' or 'how' this improvement can be more rationally made are given further, using the exergy results.

Energy efficiency deals only with energy quantities aspects, while exergy relates both quantity and quality aspects, indicating the actual 'effort' required by each component to 'produce' the 'desired product'. Being exergy a non-conservative property, significant differences are found between energy and exergy-based efficiencies. Especially for components working near dead-state conditions (ii, iii, iv and v), the exergy efficiencies are extremely low. The exergy efficiency could give hints about the most inefficient component of the plant, although this indicator alone is not enough since each component has different exergy input rates. Concerning chiller and boiler that from an energy perspective appear to be the most efficient components of plant, from an exergy point of view, they have

Table III. Exergy analysis results of the DCS, for dead-state conditions: $T_0 = 26.1\,°C$, $\omega_0 = 0.0114\,kg$ water/kg dry air and $p_0 = 101.325\,kPa$.

Plant component	Exergy input rate [kW]	Irreversibility rate [kW]	Exergy efficiency [%]	Relative Irreversibility [-]
i	0.236	0.116	50.8%	1.2%
ii	0.081	0.074	8.4%	0.8%
iii	0.138	0.135	1.6%	1.4%
iv	1.496	1.358	9.2%	13.9%
V	0.113	0.103	9.0%	1.1%
vi	0.683	0.339	50.4%	3.5%
vii	8.329	7.646	8.2%	78.2%
Overall	11.075	9.772	11.8%	100.0%

indeed very low efficiency values: 9.2% and 8.2%, respectively as shown in Table III. The overall exergy performance of the DCS was estimated as 11.8%, which indicates an even higher potential for improvement than from energy perspective.

Better than individual exergy efficiencies of components, exergy analysis techniques may also provide information about the highest contributors for plant inefficiencies, applying the concept of 'relative irreversibility' and 'exergy efficiency defect' [2,3]. The irreversibilities generated in each component of the plant are related with the exergy efficiency and the magnitude of exergy inputs rate. The exergy input rate, irreversibility rate, exergy efficiency and relative irreversibility for each component are shown in Table III. The results indicate the boiler (vii) as the component where the highest irreversibility rate occurs (7.6 kW), followed by the chiller (1.4 kW), with a relative irreversibility of 78.2% and 13.9%, respectively. As the major part of the air state points are relatively

near to the dead-state conditions, the use of high exergy sources, such as electricity for the chiller and natural gas in the boiler, leads to high levels of irreversibilities in those components.

Concerning the most inefficient component in the plant (the boiler), the irreversibilities arise mainly due to two energy conversion processes: the chemical exergy of the fuel (natural gas) when converted into thermal energy, usually evaluated at flame temperature (about 2200 K) and when the thermal energy is converted into low-temperature thermal sources (hot water). Therefore, the replacement of the boiler by a more exergy efficient technology, or that makes use of low-exergy thermal sources, may significantly contribute for the reduction of the irreversibility rates.

Besides to relative irreversibility indicator, the concept of exergy efficiency defect [3] is applied to compare the irreversibility rate at a given component and the total exergy input to the plant. The results are shown in Figure 5 and indicates that the most inefficient component of the plant (higher exergy efficiency defect) is the boiler (69.0%), followed by the chiller (12.3%) and heating coil (3.1%). The overall exergy efficiency defect is about 88.2%, indicating a huge potential for improvement. For the rational improvement of the exergy performance of the system, the exergy analysis method indicates the boiler as the first component to be replaced, since it has the highest value of exergy efficiency defect.

As previously stated, the reference state is a very important parameter for the exergy analysis. Since other alternatives for dead state could be used, the sensibility of the overall exergy efficiency of the system with the reference (dead-state) temperature was examined. As results, the exergy efficiency varies from 14% to about 8% when the reference temperature increases from 19 °C to 37 °C (292 K to 310 K). They show that for higher outdoors (reference) temperature, the margin or potential for improving the system increases, meaning the actual exergy input rate 'grow faster' than the theoretical useful exergy rate. Nevertheless, the reference humidity ratio was assumed constant (0.0114 kg/kg), therefore different results could arise if the variation of ω_0 was also taken into account.

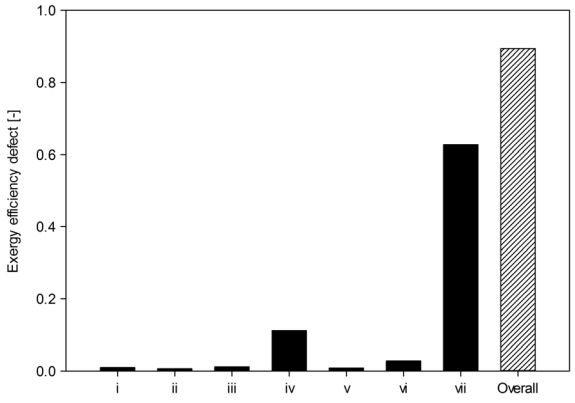

Figure 5. Exergy efficiency defect for the components (i–vii) of DCS.

4.4. Analysis of performance for different heating technologies and renewable energy sources

Alternative ways for improving the heating system exergy performance include its replacement by another technology that makes use more efficiently of primary-fossil energy resources (e.g. heat pump or cogeneration system) or use low-temperature (or low-exergy) sources, preferentially derived from renewable sources (e.g. solar thermal system or other thermal waste).

The current combustion heat generator (natural gas boiler) leads to very low-exergy performances due to high irreversibility levels that occur during the energy conversion process. Once the temperature levels required for the air regeneration are relatively moderate (less than 90 °C), the use of low-temperature thermal renewable sources is a good alternative for the heating system. However, some renewable options cannot effectively lead to improvements on exergy efficiency, although conduct reductions on primary-fossil energy demand (e.g. heating systems fuelled by wood, biofuels/biomass). In this way, to compare different alternative heating systems, primary energy and exergy performance indicators should be used. In this study, a set of different alternative heating systems technologies (including renewables) were proposed, and the indicators

Table IV. Proposed scenarios and main parameters used for the exergy analysis of DCS, concerning renewables and others heating technologies.

Scenario #	Description
A	Natural gas boiler, with thermal efficiency 90% (**original system**).
B	**Scenario A (60%) + solar thermal system (40%)**: the natural gas boiler provides 60% of the heat requirements and the solar thermal system 40%. Solar thermal supply and return temperatures: $T_s = 60$ °C and $T_r = 40$ °C, respectively. $\left(F^{ex}_{r,hs} = 0.15\right)$ [33].
C	**Scenario A (20%) + solar thermal system (80%)**: the natural gas boiler provides 20% of the heat requirements and the solar thermal system 80%. Solar thermal supply and return temperatures: $T_s = 60$ °C and $T_r = 40$ °C, respectively. $\left(F^{ex}_{r,hs} = 0.15\right)$ [33].
D	Heat requirements fully provided by a **wood-fuelled heating system**, with thermal efficiency of 86%, based on efficiency-based harmonized values [35]. Exergy to LHV of wood $\left(F^{ex}_{r,hs} = 1.05\right)$ [33].
E	Heat requirements fully provided by an **electric heating system**, with an estimated thermal efficiency of 95%.
F	Heat requirements fully provided by air source heat pump, assuming **COP = 2**.
G	Heat requirements fully provided by groud source heat pump, assuming **COP = 4**.

Int. J. Energy Res. 2014; **38**:714–727 © 2013 John Wiley & Sons, Ltd.
DOI: 10.1002/er

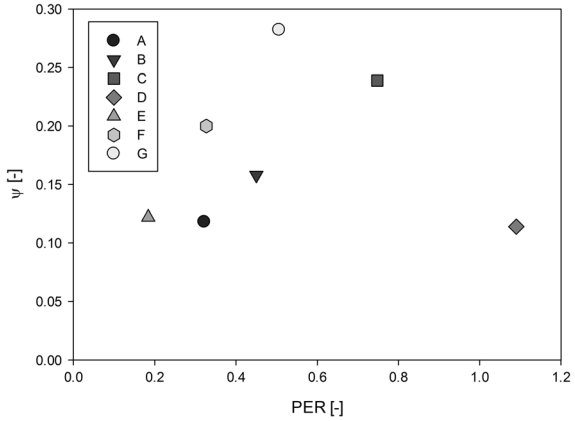

Figure 6. PER vs. exergy efficiency concerning different renewables and heating technologies scenarios.

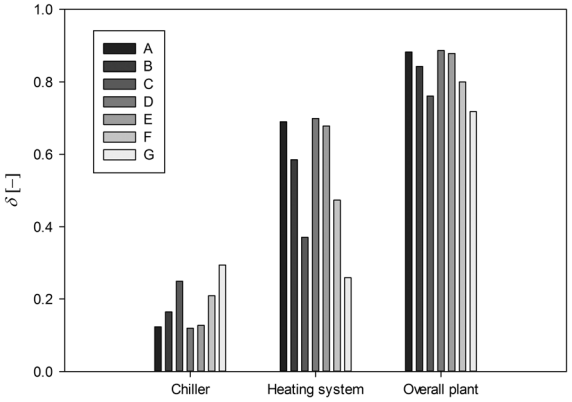

Figure 7. Exergy efficiency defect for the proposed heating systems and their impact on chiller (primary based) and overall plant.

PER and exergy efficiency were applied to compare them, keeping the cooling system as the same (i.e. chiller with an averaged COP 2.37). A brief description of the proposed scenarios and the main parameters used for each is presented in Table IV.

In Figure 6, a PER vs. exergy efficiency diagram is presented showing the differences between primary energy and exergy performance for each scenario considered. There are a couple of options that make lower use of primary-fossil energy sources, but that may not correspond to high exergy efficiency scenarios. The intensive use of renewables conducts to reductions on fossil energy sources (increasing of PER), although concerning exergy efficiency, the results show significant differences depending on the type or quality of sources used. As an example, in Scenario D, heating requirements are totally provided by wood (considered a fully renewable source). This scenario presents the highest value of PER; however, it corresponds to the lowest exergy efficient option ($\psi = 11.4\%$), because wood is a high exergy source, and the combustion process is a highly irreversible process. On the other side, Scenario G (heat pump with COP 4 as heating system) presents the highest exergy efficiency (about 27%), despite a moderate PER (50.6%). The worst PER option is the Scenario E (a purely electric heating system) that corresponds to a primary energy efficiency (PER = 20%). This is mostly related to the primary energy associated to the electricity production, leading to a low PER value. Additionally, the exergy efficiency associated to this option presents also a low value, indicating the electric resistance as an inadequate technology converting electricity (high exergy) into thermal energy (low-exergy) for air regeneration. These analyses show that the exclusive use of PER is not sufficient to describe the overall performance of DCS, and the exergy efficiency indicator reveals to be a good complementary indicator providing additional information about the rational use of energy sources.

Considering these scenarios, Figure 7 shows the variations of the parameter 'exergy efficiency defect' occurring in the two most inefficient components of the plant, the chiller, the heating system and the overall plant. The results clearly show the high exergy efficient options as C and G, which corresponds to scenarios with low exergy efficiency defect values (76.1% and 71.8%, respectively). They correspond to the best exergy performances, due to irreversibilities reductions obtained at the heating system. In these results, exergy efficiency defect is demonstrated as an important parameter that helps to identify the most inefficient component of the plant at each scenario. As an example, in the scenario A, the heating system (natural gas boiler) was responsible for 69% of exergy efficiency defect and chiller for 12.3%. The heating system was found as the most inefficient system, so its replacement by a more efficient technology could contribute for improvements on overall performance of the plant. Additionally, for the most exergy efficient option (G), the exergy efficiency defect is 25.9% for the heating system (heat pump) and 29.4% for the chiller, showing in this case that the chiller is a higher contributor for the inefficiencies than the heating system.

4.5. Operating conditions and irreversibilities savings

For the DW regeneration, depending on the outdoors conditions (temperature and humidity ratio), well-defined air

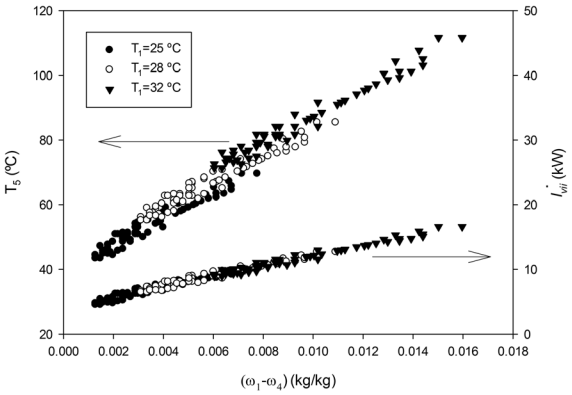

Figure 8. Regeneration temperature and irreversibility rate at boiler for three levels of inlet temperatures.

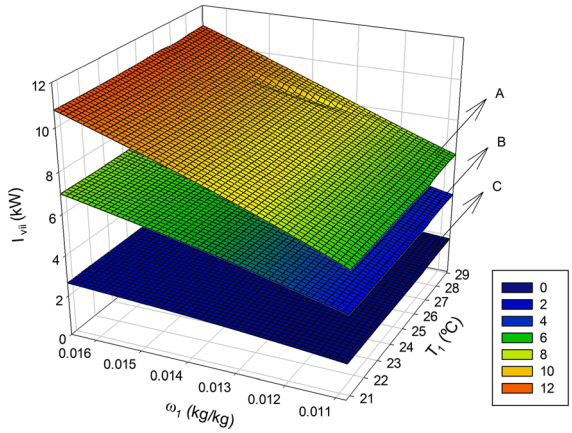

Figure 9. Irreversibility rate at heating system (vii), as function of inlet temperate and humidity ratio for scenarios A, B and C.

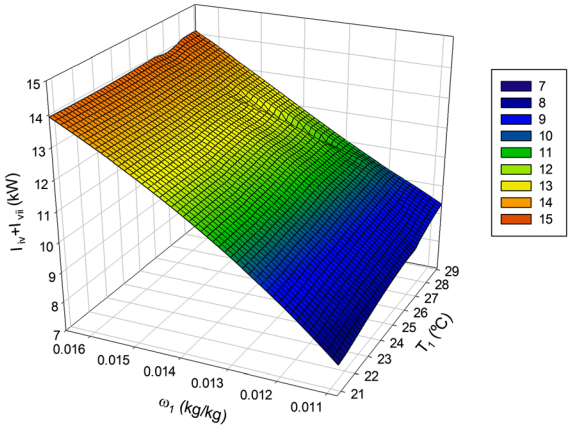

Figure 10. Sum of the irreversibility rate at boiler (vii) and chiller (iv), as function of inlet temperate and humidity ratio.

temperatures and heat loads are required. For the period of analysis, and choosing as desired output conditions $T_4 = 18$ °C and $\omega_4 = 0.008$ kg/kg, some parametric analysis was conducted for three inlet temperatures levels ($T_1 = 25$ °C, 28 °C and 32 °C) and assuming the humidity ratio occurring in the period. In Figure 8, the temperature requirements for air regeneration at point 5 and the corresponding irreversibility rate at the boiler are shown. The results show that temperature required for air regeneration (T_5) and irreversibility rate of the boiler $(\dot{I}_{vi})$ increase for higher humidity ratio and temperature differences between points 1 and 4.

Concerning the same period, in Figure 9, surfaces corresponding to the irreversibility rate occurring in scenarios A, B and C are represented as function of inlet temperature and humidity ratio, (T_1,ω_1) pairs verified in the period of analysis. For simplicity, no other scenarios were taken into account. The output desired conditions were kept constant at $T_4 = 18$ °C and $\omega_4 = 0.008$ kg/kg. Similarly, the results show that irreversibility rate rises for increasing values of T_1 and ω_1. Comparing the scenarios A, B and C, the lowest irreversibility rate is obtained when high share of solar thermal is used for the heating system. In this example, the quality factor associated to low-temperature solar thermal sources is $F^{ex}_{r,hs} = 0.15$, calculated based on supply and return temperatures of 60 °C and 40 °C, respectively [33]. For these temperature levels, solar thermal systems alone could not be enough for DW regeneration, especially for high-temperature requirements. Therefore, these systems have to be integrated with other technological systems able to deliver heat at adequate temperature levels for the regeneration process.

In Figure 10, the sum of the irreversibility rate occurring at the two most inefficient sub-systems (the chiller and the boiler at scenario A) is represented as function of humidity ratio and inlet temperature. Considering the same output desired conditions, $T_4 = 18$ °C and $\omega_4 = 0.008$ kg/kg, the results show that the irreversibilities levels are more sensible to variations of inlet humidity ratio than of inlet temperature levels.

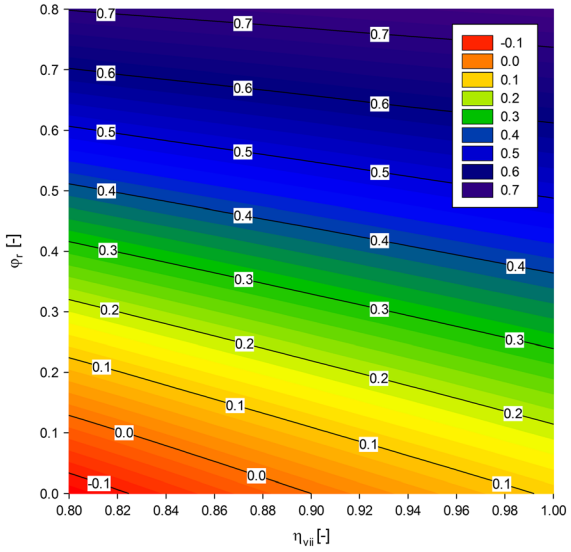

Figure 11. Relative irreversibilities savings due to integration of renewables from solar thermal.

The RIS between heating systems can be shown by changing different parameters through the use of iso-line diagrams. In Figure 11, considering Scenario A as reference, RIS is shown as function of boiler efficiency and share of solar thermal renewable sources, assuming $F^{ex}_{r,hs} = 0.15$. The results show that improvements on heating efficiency or fraction of renewable thermal sources lead to reductions of the irreversibility rates, leading to the increase of irreversibility differences between reference and alternative system. As an example, from Figure 11, the best represented scenario ($\eta_{vii} = 1$ and $\phi_r = 0.8$) corresponds to a RIS of about 75%.

5. CONCLUSIONS

In this paper, an energy and exergy analysis was applied for a novel, non-conventional DCS, in order to locate and

Int. J. Energy Res. 2014; **38**:714–727 © 2013 John Wiley & Sons, Ltd.
DOI: 10.1002/er

quantify the most inefficient sub-components of the plant. The overall primary energy performance of the DCS, using the indicator PER was estimated as 32% and the exergy performance 18.8%. PER provides information about the conversion efficiency of the primary energy requirements of the plant taking into account the useful energy delivered. The resultant value (32.2%) shows a great potential for improvement, which could be accomplished by replacing the primary energy inputs of the boiler and chiller by renewable energy sources or using higher efficient systems. The exergy performance includes quantity and quality energy aspects, being a thermodynamic more detailed indicator. Since the "output product" (moist air flow) is delivered at temperature relatively close to the reference state, its exergy performance tend to be low. In this case, to improve the exergy performance is needed to use sources more compatible with the exergy output levels, which if they are from renewable sources also improves PER – the ideal scenario. Using the parameter exergy efficiency defect, the results indicate the boiler as the most inefficient component of the plant (69%), followed by the chiller (12.3%). The other components are relatively insignificant for the total irreversibilities of the plant.

The replacement of the natural gas boiler by alternative heating technologies, such as, low-temperature solar thermal renewable sources or high efficient heat pump systems are those that mostly improve the DCS exergy performance. The results also show that the use of renewables reduces effectively the primary energy demand of the plant, although does not always correspond to the best exergy scenario. For a complete and detailed assessment, both primary energy-based indicators (PER) and exergy efficiency should be used. From the examples, the wood-fuelled heating system has the highest value in terms of PER (107.2%), but it is the lowest exergy efficient option (11.4%). On the other side, the heat pump system (COP = 4) is the heating system with the highest exergy efficiency (about 27%), but with a moderate PER value (50.6%). The effectiveness of the exergy method for analysis is demonstrated through this paper, where the exergy efficiency defect was found as a helpful method to assess and locate high sources of irreversibilities, showing the direction to minimize exergy losses and to approach the ideal system. Moreover, the irreversibility rate was found as highly dependent on inlet conditions; therefore, for fixed outlet conditions, the maximum irreversibility rate value was obtained for high temperature and humidity ratio differences between inlet and outlet conditions.

NOMENCLATURE

$\dot{C}_{\min}$ = Minimum of the capacitance rate [kJ K^{-1} s^{-1}]
$c_{p,a}$ = Specific heat at constant pressure of dry air [kJ kg^{-1} K^{-1}]
$c_{p,v}$ = Specific heat at constant pressure of water vapour [kJ kg^{-1} K^{-1}]
COP = Coefficient of performance [-]
$\dot{E}_p$ = Primary-fossil energy input rate [kW]
$\dot{E}_r$ = Renewable energy input rate [kW]
ex = Specific exergy of moist air [kJ kg^{-1}]
$\dot{E}x$ = Exergy rate [kW]
ex_{ch} = Specific chemical exergy of mixture [kJ kg^{-1}]
ex_{tm} = Specific thermo-mechanical exergy of mixture [kJ kg^{-1}]
ex_w = Specific exergy of water [kJ kg^{-1}]
F_{el}^{p} = Primary energy factor for electricity [-]
F_{f}^{ex} = Chemical exergy to Lower Heating Value (LHV) of the fuel [-]
F_{r}^{ex} = Quality factor associated to the renewable energy source used [-]
h = Specific enthalpy [kJ kg^{-1}]
h_f = Specific enthalpy of saturated-liquid (water) [kJ kg^{-1}]
h_{fg} = Enthalpy of vaporization for water [kJ kg^{-1}]
$\dot{I}$ = Irreversibility rate [kW]
I_R = Relative irreversibility [-]
$\dot{m}_{a,C}$ = Mass air flow rate for air stream C [kg s^{-1}]
$\dot{m}_{a,P}$ = Mass air flow rate for air stream P [kg s^{-1}]
$\dot{m}_{a,R}$ = Mass air flow rate for air stream R [kg s^{-1}]
$\dot{m}_{cw}$ = Mass flow rate of chilled water [kg s^{-1}]
$\dot{m}_{hw}$ = Mass flow rate of hot water [kg s^{-1}]
$\dot{m}_w$ = Water mass flow rate for the evaporative cooler [kg s^{-1}]
p = Pressure [kPa]
p_{sat} = Saturated pressure [kPa]
PER = Primary energy ratio [-]
$\dot{Q}_{reg}$ = Heat rate required for air regeneration [kW]
R_a = Ideal gas constant of dry air [kJ kg^{-1} K^{-1}]
R_v = Ideal gas constant of water vapour [kJ kg^{-1} K^{-1}]
RIS = Relative irreversibilities savings [-]
s = Specific entropy [kJ kg^{-1} K^{-1}]
s_f = Specific entropy of saturated liquid (water) [kJ kg^{-1}]
T = Temperature [°C] or [K]
T_w = Wet-bulb temperature [K]
v_f = Specific volume of saturated liquid (water) [m^3 kg^{-1}]
$\dot{W}_{el}$ = Electricity input rate [kW]
y_i = Molar fraction of a substance i in the mixture [-]

Greek symbols

ϵ = Effectiveness [-]
δ = Exergy efficiency defect [-]
φ = Relative humidity [-]
ϕ_r = Fraction of heat produced from renewables [-]
η_{eg} = Averaged electric grid efficiency [-]
η_{hs} = Thermal efficiency of heating system
μ_i = Chemical potential of the substance i [kJ kg^{-1}]
ψ = Exergy efficiency [-]
ω = Humidity ratio [kg kg^{-1}]

Subscripts

0	=	Restricted dead state
hs	=	Heating system.
in	=	Input or required
j	=	Assessment point
k	=	Component
out	=	Output or desired
ove	=	Overall
r	=	Return
ref	=	Reference scenario
s	=	Supply

Acronyms

DCS	=	Desiccant cooling system
DW	=	Desiccant wheel

ACKNOWLEDGEMENTS

The authors acknowledge the support received from the Foundation for Science and Technology of the Portuguese Ministry of Education and Sciences, through the MIT PORTUGAL Program, grant no. SFRH/BD/51018/2010, and Università degli Studi del Sannio for the additional support provided.

REFERENCES

1. Bejan A. *Advanced engineering thermodynamics* (3rd). Wiley & Sons: Hoboken, 2006.
2. Moran M, Shapiro H. *Fundamentals of Engineering Thermodynamics* (6th). Wiley & Sons: Hoboken, 2008.
3. Kotas TJ. *The exergy method of thermal plant analysis* (1st). Krieger: Malabar, 1995.
4. Dinçer I, Rosen MA. *Exergy: energy, environment, and sustainable development* (1st). Elsevier: Amsterdam, 2007.
5. Angrisani G, Minichiello F, Roselli C, Sasso M. Desiccant HVAC system driven by micro-CHP: Experimental analysis. *Energy and Buildings* 2010; **42**(11):2028–2035.
6. Angrisani G, Minichiello F, Roselli C, Sasso M. Experimental investigation to optimise a desiccant HVAC system coupled to a small size cogenerators. *Applied Thermal Engineering* 2011; **31**(4):506–512.
7. Angrisani G, Roselli C, Sasso M. Experimental validation of constant efficiency models for the subsystems of an unconventional desiccant-based Air Handling Unit and investigation of its performance. *Applied Thermal Engineering* 2012; **33-34**:100–108.
8. Angrisani G, Capozzoli A, Minichiello F, Roselli C, Sasso M. Desiccant wheel regenerated by thermal energy from a microcogenerator: Experimental assessment of the performances. *Applied Energy* 2011; **88**(4):1354–1365.
9. Klein SA. TRNSYS Version. 17. Solar Energy Laboratory, University of Wisconsin-Madison, 2010.
10. Parmar H, Hindoliya DA. Artificial neural network based modelling of desiccant wheel. *Energy and Buildings* 2011; **43**(2011):3505–3513.
11. La D, Dai Y, Li Y, Ge T, Wang R. Study on a novel thermally driven air conditioning system with desiccant dehumidification and regenerative evaporative cooling. *Building and Environment* 2010; **45**(11):2473–2484.
12. Hao X, Zhang G, Chen Y, Zou S, Moschandreas DJ. A combined system of chilled ceiling, displacement ventilation and desiccant dehumidification. *Building and Environment* 2007; **42**(9):3298–3308.
13. Chun W, Oh SJ, Lim SH, Chen K. Maximum efficiency of solar energy conversion. *International Journal of Energy Research* 2012; **36**:928–934.
14. Roux WG, Ochende TB, Meyer JP. Thermodynamic optimisation of the integrated design of a small - scale solar thermal Brayton cycle. *International Journal of Energy Research* 2012; **36**:1088–1104.
15. Balli O, Aras H, Hepbasli A. Exergetic performance evaluation of a combined heat and power (CHP) system in Turkey. *International Journal of Energy Research* 2007; **31**:849–866.
16. Gonçalves P, Gaspar A, Silva MG. Comparative exergy and energy performance analysis of a separated and combined heat and power system for a student housing building. In *Proceedings MICRoGEN II: 2nd International Conference on Microgeneration and Related Technologies. Glagow, 4-6 April* 2011.
17. Gonçalves P, Gaspar AR, Silva MG. Energy and exergy-based indicators for the energy performance assessment of a hotel building. *Energy and Buildings* 2012; **52**:181–188.
18. Sakulpipatsin P, Itard LCM, van der Kooi HJ, Boelman EC, Luscuere PG. An exergy application for analysis of buildings and HVAC systems. *Energy and Buildings* 2010; **42**:90–99.
19. Khennich M, Galanis N. Thermodynamic analysis and optimization of power cycles using a finite low - temperature heat source. *International Journal of Energy Research* 2012; **36**:871–885.
20. Darwish NA, Gadalla MA. Performance assessment of a liquid-phase separation refrigeration cycle. *International Journal of Energy Research* 2012; **36**:1183–1191.
21. Dincer I, Hussain MM, Al-Zaharnah I. Analysis of sectoral energy and exergy use of Saudi Arabia. *International Journal of Energy Research* 2004; **28**(3):205–243.

22. Wei Z, Zmeureanu R. Exergy analysis of variable air volume systems for an office building. *Energy Conversion and Management* 2009; **50**(2):387–392.
23. U.S. DOE, EnergyPlus Energy Simulation Software. 2012. Available: http://apps1.eere.energy.gov/buildings/energyplus. [Accessed: 27-03-2012].
24. Lavan WM, Monnier Z, Worek Z. Second law analysis of desiccant cooling systems. *ASME Journal of Solar Energy Engineering* 1986; **104**:229–236.
25. Kanoglu M, Çarpınlıoğlu MÖ, Yıldırım M. Energy and exergy analyses of an experimental open-cycle desiccant cooling system. *Applied Thermal Engineering* 2004; **24**(5):919–932.
26. Hürdoğan E, Buyükalaca O, Hepbasli A, Yılmaz T. Exergetic modeling and experimental performance assessment of a novel desiccant cooling system. *Energy and Buildings* 2011; **43**(6):1489–1498.
27. Ahmed CSK, Gandhidasan PS, Zubair M, Al-Farayedhi AA. Exergy analysis of a liquid-desiccant-based, hybrid air-conditioning system. *Energy* 1998; **23**(1): 51–59.
28. Xiong ZQ, Dai YJ, Wang RZ. Development of a novel two-stage liquid desiccant dehumidification system assisted by CaCl2 solution using exergy analysis method. *Applied Energy* 2010; **87**(5): 1495–1504.
29. Wang L, Li N, Zhao B. Exergy performance and thermodynamic properties of the ideal liquid desiccant dehumidification system. *Energy and Buildings* 2010; **42**(12):2437–2444.
30. Angrisani G, Roselli C, Sasso M, Stellato C. Design and simulation of a solar assisted desiccant-based air handling unit. In *Proceedings 8th International Conference on Heat Transfer, Fluid Mechanics and Thermodynamics*, July 11–13. Pointe Aux Piments, Mauritius, 2011.
31. Ertesvåg IS. Exergetic comparison of efficiency indicators for combined heat and power (CHP). *Energy* 2007; **32**:2038–2050.
32. Angrisani G, Roselli C, Sasso M. Distributed microtrigeneration systems. *Progress in Energy and Combustion Science* 2012; **38**:502–521.
33. Annex 49, Low Exergy Systems for High-Performance Buildings and Communities. ECBCS-IEA, 2010.
34. Klein SA. Engineering Equation Solver (EES). F-Chart Software, 2004.
35. European Commission. Harmonized efficiency reference values for separate production of electricity and heat in application of Directive 2004/8/, Official Journal of the European Union 21 December 2006, 6.2.2007: L 32/ 183-L 32/188.